

## 8.1 Introduction

Energy conservation is an energetic issue for the societies at present-day. Therefore, enhancement in the thermal efficiency of both industrial and residential buildings becomes necessary. Hence, numerous researches around the globe are engaged to find the best route of energy saving in the building sector and several concepts have come out for the same (Dan *et al.*, 2016). Nowadays, application of room heater and air conditioner increases in the buildings to retain ambient temperature, but this maintenance of ambient temperature can't remain stable due to high heat flow through walls and roofs of the buildings. Therefore, the application of high performance thermal insulating materials for the inner lining of rooms can effectively reduce the energy losses which occur due to building walls and roof (Zhang *et al.*, 2014). However, all type of inner lining materials is presently manufactured by the combinations of locally available natural ingredients like reactive quartz sand or diatomaceous earth as siliceous material, limestone or ordinary portland cement (OPC) as calcium material and different fiber materials for reinforcing followed by mixing, shaping and curing at a different temperatures or sintering at high temperature (Chen *et al.*, 2017; Heriyanto *et al.*, 2018). The huge use of virgin raw materials for the production of building material has caused an enhancement in the deficit level of the natural resources, which is already present in a low amount. For both the aspects, i.e., energy consumption and alternative raw material, many researchers explore a different type of building materials for their studies. Wang *et al.* (2018) and Ji *et al.* (2017) have synthesized the energy-saving composite (dense/foam bi-layered) board by fly ash and other ceramic wastes. Hurtado *et al.* (2014) have produced calcium silicate insulating masonry units by adding bottom ash 10 to 90 wt.% in the composition.

This study explores a new approach to investigate the possibility of utilization of fly ash and seashells as alternative ingredients in the composition of the ceramic board (CB) that mostly uses virgin raw materials. The room temperature curing process is used to fabricate the board specimens through the mixing of a small amount (10 wt.%) of OPC. Unground rice

husk ash (URHA) (without heat-treated) and rice husk (RH) are used as reinforcement's media in CB. The physical, thermal and mechanical properties of the waste-derived CB samples are comprehensively investigated, and the effect of humidity on the mechanical property is also briefly discussed.

## **8.2 Experimental procedure**

### **8.2.1 Ceramic powder synthesis**

The preparation flow chart of multi-phase ceramic powder (MCP) and CB is shown in [Figure 8.1](#). The MCP was synthesized through a solid-state reaction method using 1:1 weight ratio of fly ash and heat-treated seashell as ingredients. Two respective powders were wet ball-milled in water media for 4 h with 600 rpm. Milled mass was dried at 110°C and calcination was done at 1100°C for 4 h in an air atmosphere. Later, the agglomerated calcined particles were dry milled for 1 h with 600 rpm.

### **8.2.2 Ceramic board synthesis**

The most facile and economical room temperature curing process was used to fabricate the CB specimens. The batch composition and sample's nomenclature are shown in [Table 8.1](#). All the raw materials were mixed in a dry condition as per batch composition for about 20 min, and then the 15 wt.% of water was mixed for casting followed by mixing for 10 min. The wet mix was transferred into properly oiled different shape ( $70 \times 70 \times 6 \text{ mm}^3$ ,  $25 \times 25 \times 5 \text{ mm}^3$  and  $40 \times 10 \times 6 \text{ mm}^3$ ) steel mould, and a flat surface was prepared by vibro-caster for about 10 min. Then, the specimens were cured at room temperature for about 24 h (without autoclave). After that, the samples were taken out from the mould, and resulting specimens were taken to cure at room temperature in a humid chamber (70-90% relative humidity) for 7 days. For appropriate results, six specimens of each composition were prepared, and all the testing was done after the drying of the samples at 50°C.



**Figure 8.1** Preparation flowchart of ceramic board specimens.

**Table 8.1** Sample's nomenclature and composition.

Ingredients (wt.%)	s-1	s-2	s-3	s-4	s-5	s-6	s-7	s-8	s-9
MCP	100	90	80	75	70	85	80	75	75
URHA	0	0	10	15	20	0	0	0	10
RH	0	0	0	0	0	5	10	15	5
OPC	0	10	10	10	10	10	10	10	10

### 8.3 Results and discussion

#### 8.3.1 Characterization of MCP

Seashells contain around ~56 wt.% of solid mass (98.85 wt.% CaO) and the remaining mass is removed after the temperature of 900°C (Figure 3.3(c)). Consequently, in this study calcined seashell is used as a CaO source. Generally, the probability of unreacted CaO in the MCP system will increase with using off without calcined seashell in the fabrication process.

It may be happened due to the high amount of volume loss from seashell (~44 wt.%) decreased the contact area in-between of fly ash and CaO and create an uneven mixture. Therefore, the diffusion reaction for MCP formation at 1100°C is inhibited and some amount of CaO is present in a free state. This free CaO is harmful for the durability of CB because CaO transforms into portlandite [Ca(OH)<sub>2</sub>] when contact with water through the reaction of  $CaO + H_2O = Ca(OH)_2$ . Additionally, 98% of volume expansion occurs during this transformation, and it is introduced a tensile strength in the body (Tang *et al.*, 2017). Therefore, the crack is generated during the fabrication of CB (free CaO containing) samples, as shown in Figure 8.2. However, the separate calcination step for seashell can be skipped through the use of different type of MCP formulation furnaces, i.e., cement kiln or rotary kiln. In these types of kilns mixing and heating are done simultaneously. It will consume less amount of energy and reduce the possibility of free CaO in the MCP.

Figure 8.3 displays the DTA-TGA curve for the MCP formulation in a weight ratio of calcined seashell and fly ash (1:1). TGA curve shows a little weight loss up to 1200°C, i.e., about 1.5 wt.% due to the use of calcined seashell and low volatile containing fly ash (2.64 wt.%). However, the first small weight reduction (0.42 wt.%) is observed in the range of 400 to 500°C due to the transformation of portlandite [Ca(OH)<sub>2</sub>] to CaO, and it is attributed an endothermic peak centered at 467°C. The next weight loss is occurred from 550 to 820°C through the combination of effect in fly ash. It may be the decomposition of carbonate, combustion of unburned material and the dehydroxylation of the silicates. Therefore, the DTA curve shows a wide range of endothermic peak in this temperature range. In addition, the exothermic peaks without weight loss at around 930-1050°C are detected due to the formation of silicates, i.e., calcium silicate, aluminum silicate (Leite *et al.*, 2017). This result indicates that the calcination temperature for the MCP formation is above 1050°C.

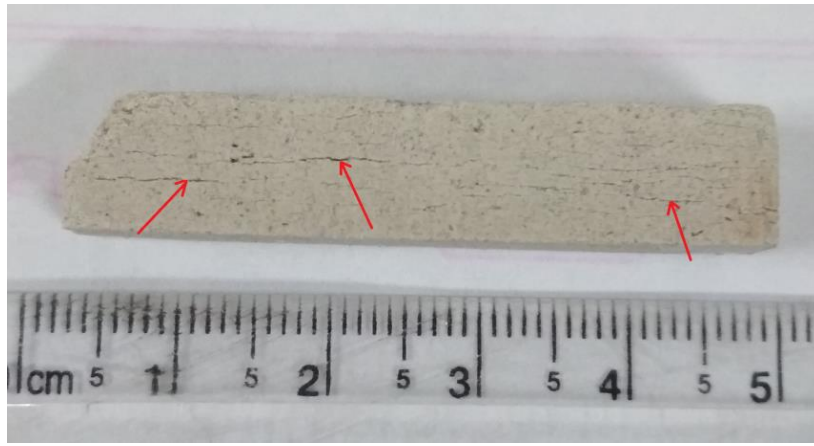


**Figure 8.2** Free CaO containing MCP derived ceramic board sample.

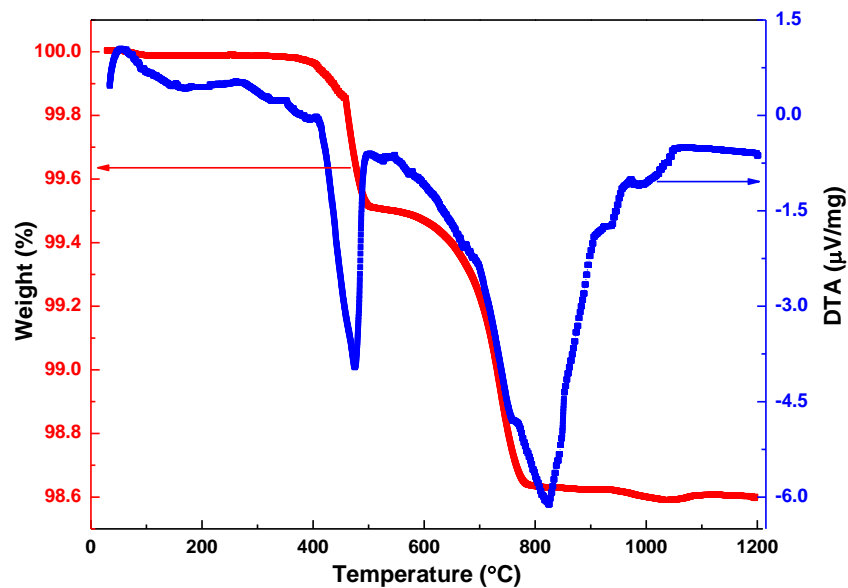


**Figure 8.3** DTA-TGA curve of multi-phase ceramic powder formulation.

Figure 8.4(a) represents the powder XRD analysis of milled MCP powder at room temperature. It confirms the formation of several phases in the system; analyzed with the help of “JCPDS-International Centre for Diffraction Data Cards.” Larnite ( $\text{Ca}_2\text{SiO}_4$ , monoclinic, space group number & name: 14, P21/n) is a major phase; and minor phases are mullite ( $\text{Al}_{4.56}\text{Si}_{1.44}\text{O}_{9.72}$ ), calcium aluminate ( $\text{Ca}_3\text{Al}_2\text{O}_6$ ) and anorthite ( $\text{CaAl}_2\text{Si}_2\text{O}_8$ ) in MCP powder. Other phases, like unreacted CaO and  $\text{SiO}_2$  could not be detected by XRD in MCP. It may be happened due to active CaO in a calcined seashell, and the active  $\text{SiO}_2$  or  $\text{Al}_2\text{O}_3$  in fly ash are energetically reacted with each other and formed new compounds. The formation of different chemical bonds during calcination at  $1100^\circ\text{C}$  is detected through FTIR analysis, which is shown in Figure 8.4(b). The absorption band in the region of  $1000\text{--}1230\text{ cm}^{-1}$  is ascribed to

the stretching vibration of Si-O-Si in [SiO<sub>4</sub>]-tetrahedra (Chen *et al.*, 2010). A group of absorption bands at 423, 610 and 985 cm<sup>-1</sup> are recognized as the formation of crystalline Ca<sub>2</sub>SiO<sub>4</sub> (Beaudoin *et al.*, 2008). Furthermore, a weak peak situated at 700 cm<sup>-1</sup> is suggested to Ca-O-Al-O-Si connections (Sembiring *et al.*, 2016). Another strong band is detected at 858 cm<sup>-1</sup>, which confirms the formation of mullite (Sembiring *et al.*, 2014). The existence of Ca-O bonds in the structure, i.e., [CaO<sub>6</sub>]-octahedra is confirmed by the peak at 423-450 and 940 cm<sup>-1</sup>; and the bending vibrations of bridge and non-bridge of Si-O group are assigned by the 600-450 cm<sup>-1</sup> spectrums (Sharafabadi *et al.*, 2017; Paluszkiwicz *et al.*, 2008). These peaks justify the formation of different phases in calcined powder at 1100°C.

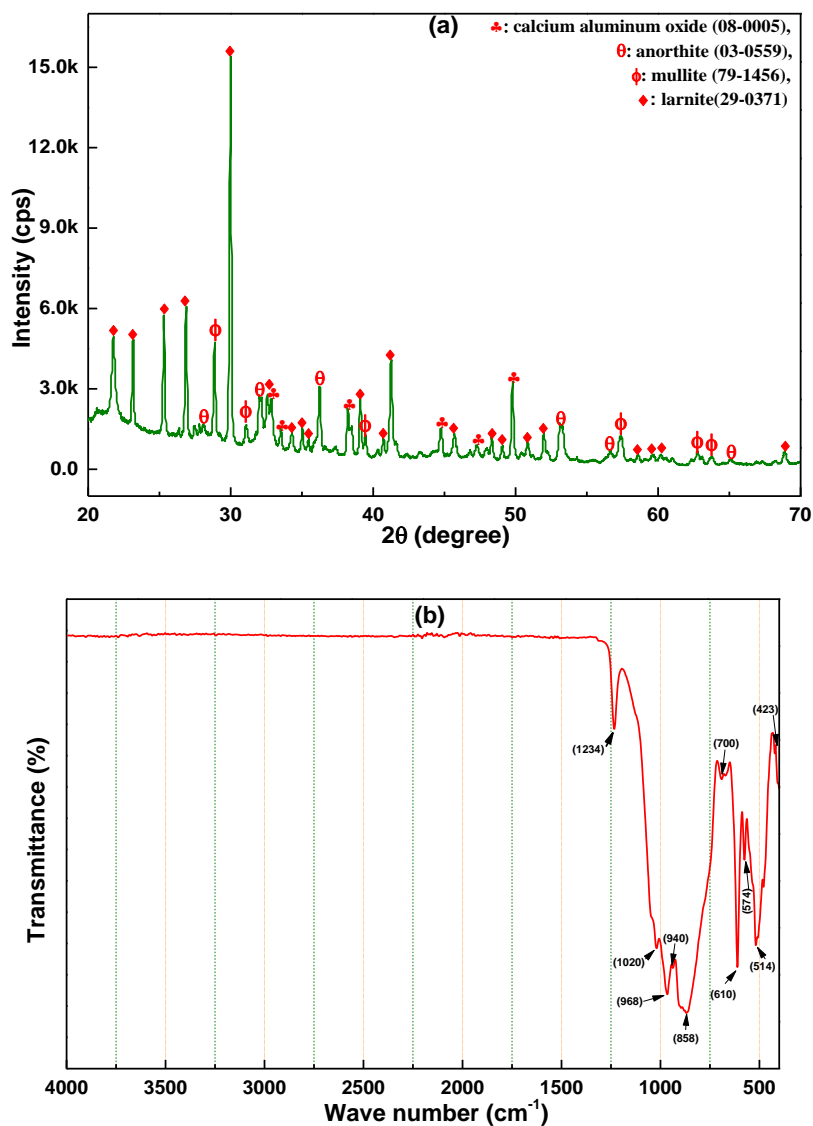


**Figure 8.4** (a) XRD and (b) FTIR analysis of multi-phase ceramic powder.

Figure 8.5(a) shows the SEM micrograph of calcined MCP after grinding. SEM analyses indicate that the powders are composed mostly of irregular or no preferential shape. Average particle size is around 0.60  $\mu\text{m}$ . The EDX analysis of the calcined powder is performed to find out the elemental and quantitative composition. Figure 8.5(b) shows the EDX analysis of MCP. It specifies the quantitative existence of O, Al, Si, Ca, Fe and Ti elements with approximately in their respective proportions in MCP.

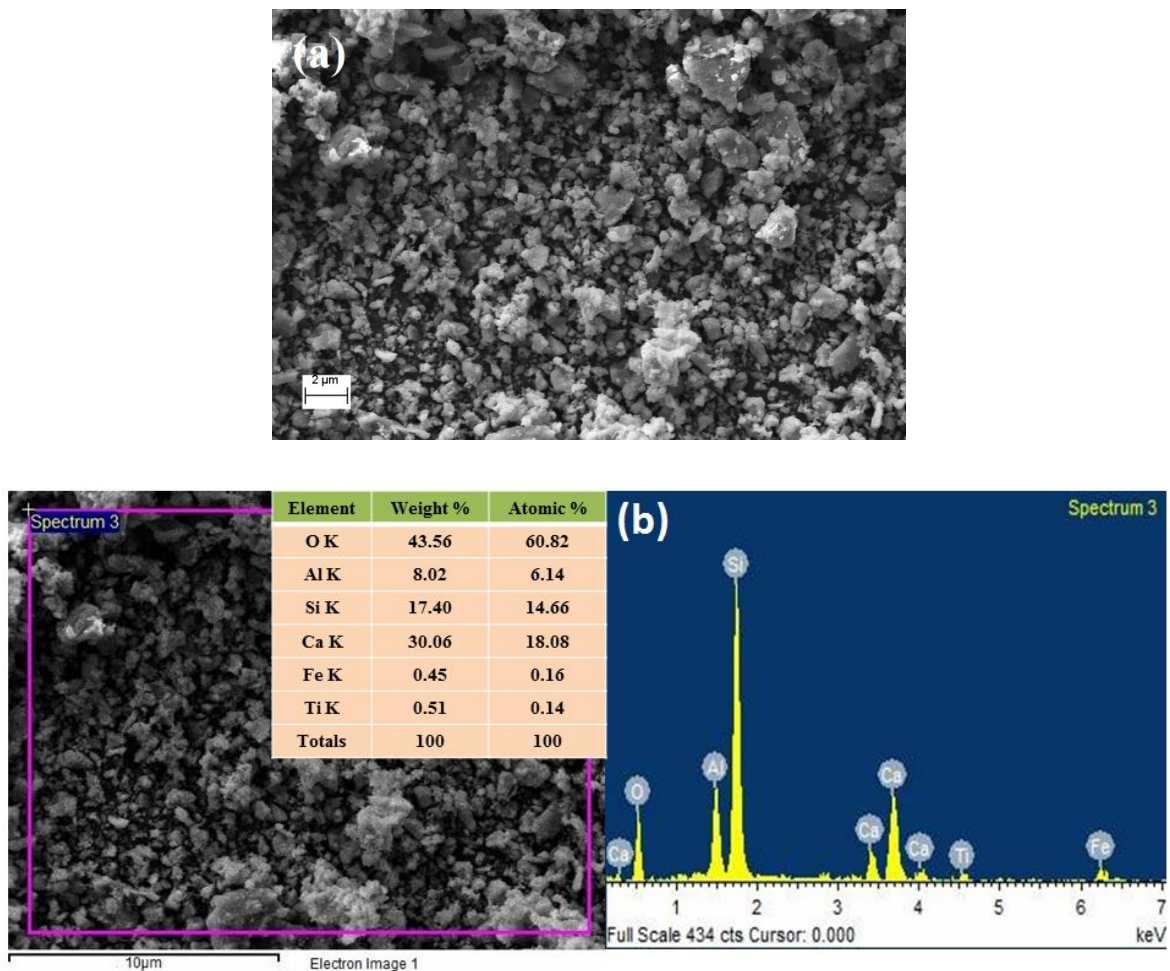
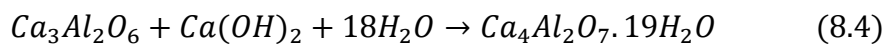
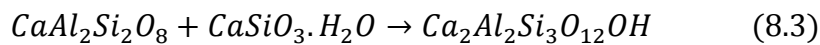
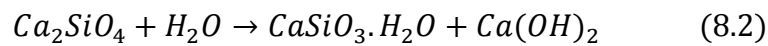
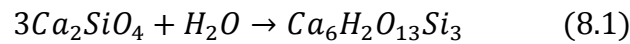


Figure 8.5 (a) SEM and (b) EDX analysis of multi-phase ceramic powder.

### 8.3.2 Characterization of ceramic board

Board samples are prepared using MCP, OPC, and RHA or RH as reinforcing materials by room temperature curing method. The key hydration products of CB are calcium silicate hydrate (C-S-H) and calcium aluminum silicate hydrate (C-S-A-H), which are responsible for achieving a practical strength of CB (Cao *et al.*, 2015). The formation of C-S-

H or C-S-A-H in CB is confirmed by the XRD analysis. [Figure 8.6](#) shows the room temperature XRD image of s-1 (only MCP) and s-2 (90%MCP+10%OPC) samples after 7 days of curing. Calcium silicate hydrate ( $\text{Ca}_6\text{H}_2\text{O}_{13}\text{Si}_3$ , anorthic, space group number & name: 2, P-2) is a main hydrated product and tanzanite ( $\text{Ca}_2\text{Al}_2\text{Si}_3\text{O}_{12}\text{OH}$ ), calcium aluminum oxide hydrate ( $\text{Ca}_4\text{Al}_2\text{O}_7 \cdot 19\text{H}_2\text{O}$ ); and small amount unreacted mullite and larnite are another phases in CB. These phases are generated through the hydration of MCP and OPC ([Eq. 8.1 to 8.4](#)). Comparing the XRD patterns, we can observe that the intensity of crystalline hydration products has slightly increased as an effect of OPC addition. It may happen due to OPC, which has high activeness for hydration than MCP. The chemical equation of this hydration process has been proposed by the following reactions:



These hydration products form a composite with unreacted mullite, larnite and other reinforcing media (RHA or RH), as graphically represented in [Figure 8.7](#) for s-9 sample. Here, hydration products such as C-S-H and C-S-A-H acts like a matrix and others (unreacted compound, RHA, and RH) are reinforced media. Therefore, the mechanical strength is increased in the CB.

[Figure 8.8](#) depicts the FTIR pattern of room temperature curing ceramic board samples (s-1 and s-2). The wide range of band around  $3600\text{-}2900\text{ cm}^{-1}$  and  $1700\text{-}1500\text{ cm}^{-1}$  is ascribed to the stretching and bending vibrations of OH groups in hydration products, respectively ([Liu et al., 2014](#); [Wang et al., 2018b](#)). The peak around  $1442\text{ cm}^{-1}$  relates to the presence of Ca-O vibration in the structure ([More et al., 2014](#)). The other peaks in the spectrum are discussed earlier in ‘characterization of MCP’ section for [Figure 8.4\(b\)](#).



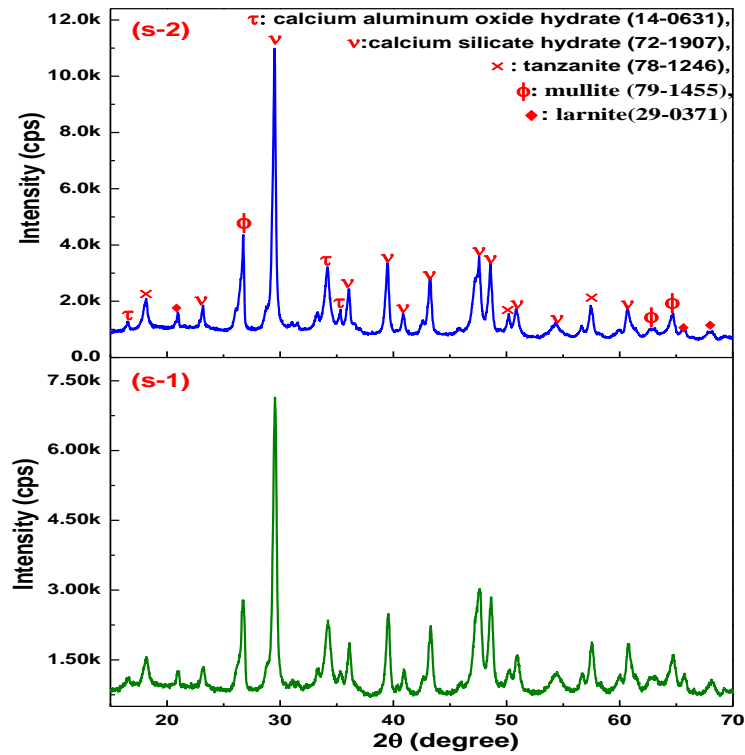


Figure 8.6 XRD analyses of s-1 and s-2 ceramic board specimens.

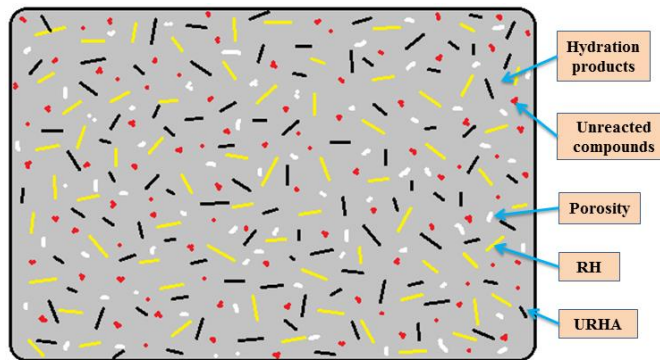


Figure 8.7 Graphical image of s-9 ceramic board sample.

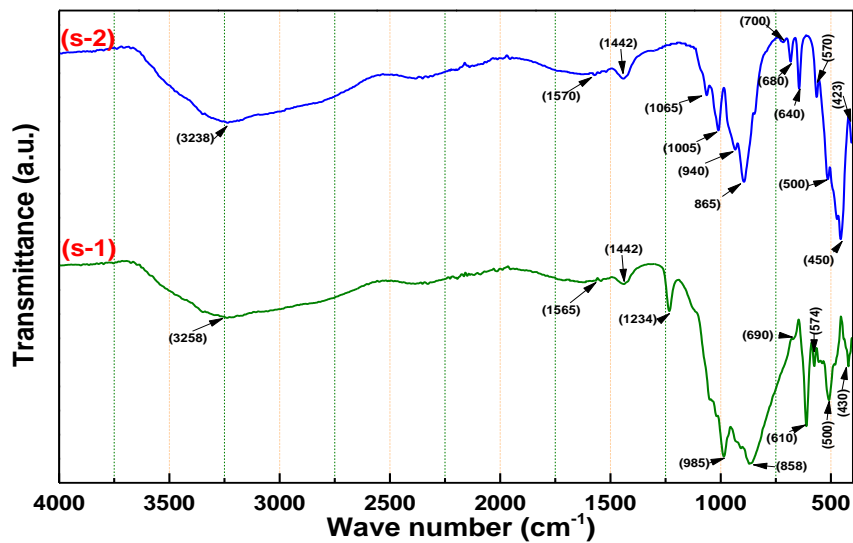
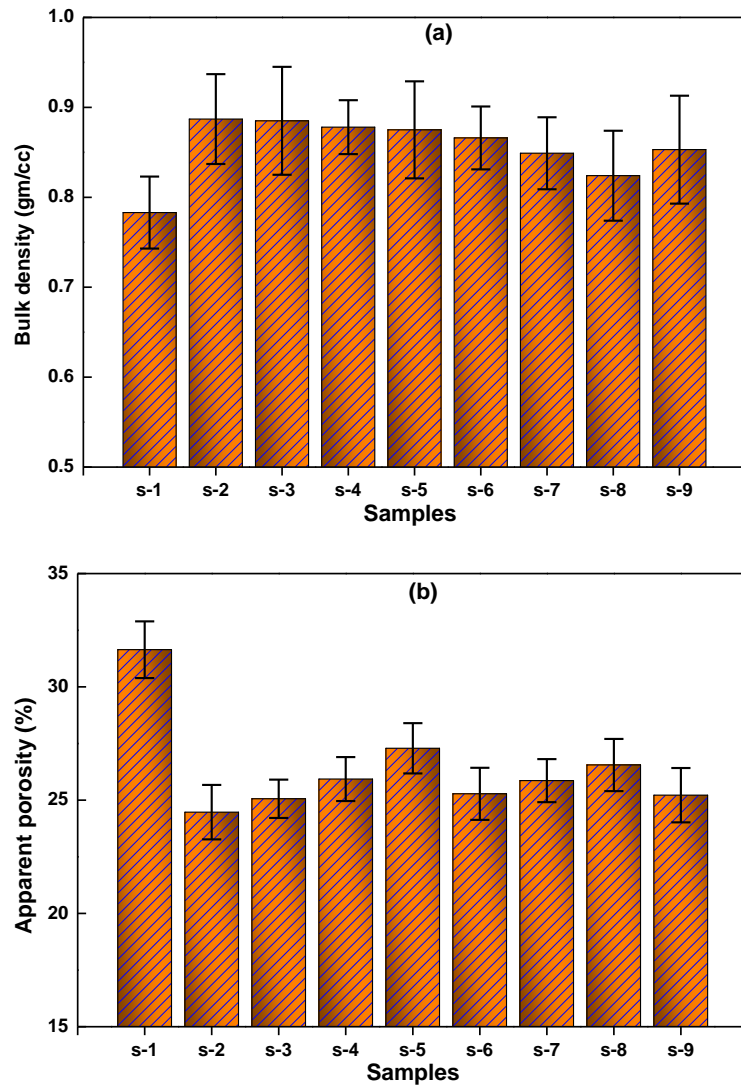


Figure 8.8 FTIR analyses of s-1 and s-2 ceramic board specimens.

The density of ceramic boards is very important with regards to the performance and specifying the applications of the material. Consequently, insulating properties (thermal conductivity) of CB very much depend on the porosity present in the board. The bulk density (BD) and apparent porosity (AP) measurements are done for all curing specimens and mean values are shown in [Figure 8.9\(a\)](#) and [\(b\)](#), respectively. It has been observed that the BD is slightly increased with the incorporation of OPC in the composition, while at the same time AP shows a little reduction. BD increases from 0.783 gm/cc to 0.887 gm/cc, and AP is decreased from 31.64% to 24.47% with the addition of 10 wt.% OPC in the system. It may ascribe due to the formation of more amounts of hydration products ([Figure 8.6](#)), which forms a higher number of cementing network. It can help to get closer the particles to each other. Subsequently, URHA does not expressively influence the AP and BD. On the other hand, RH addition faintly affects the BD, which may attribute to the light weight of this organic fiber ([Thakur and Gupta, 2006](#)). However, all the CB samples are demonstrated lower density than water (1 gm/cc), as practically represented in [Figure 8.10](#). It has been seen that the sample is floated on the water but after some time it sinks in the water because the sample absorbs water through the open pores.

The moisture absorption from atmosphere and expansion in water significantly affects the durability and quality of the board. The moisture absorption is closely related to the open porosity and size of pores in the board specimens ([More et al., 2014](#)). The mean values of water absorption and expansion in water of CB samples are illustrated in [Table 8.2](#). It can be observed that the value of water absorption decreases from 26.36 wt.% to 18.76 wt.% with OPC addition. It may be occurred due to the detracting of open porosity ([Figure 8.9\(b\)](#)). The URHA addition doesn't affect the water absorption and expansion because of it's a fired ingredient. However, RH in the composition drastically enhances these values. It can be ascribed through the absorption of water by the RH grains, having nature to absorb water. [Thakur and Gupta \(2006\)](#) have reported the diffusion coefficients of moisture in RH, i.e., 8.42

$\times 10^{-9} \text{ m}^2/\text{s}$  and moisture gain around 95 wt.% of husk after 2 h soaking in water at 30°C. Therefore, this absorption is attributed to volume growth of RH grains and enlarged the total volume of CB specimen. This behaviour of RH is harmful for durability of CB.



**Figure 8.9** (a) Bulk density and (b) apparent porosity of ceramic board specimens.

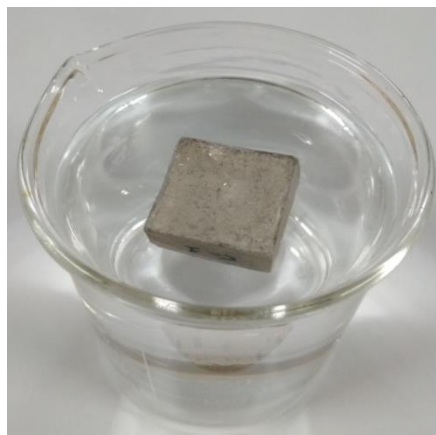
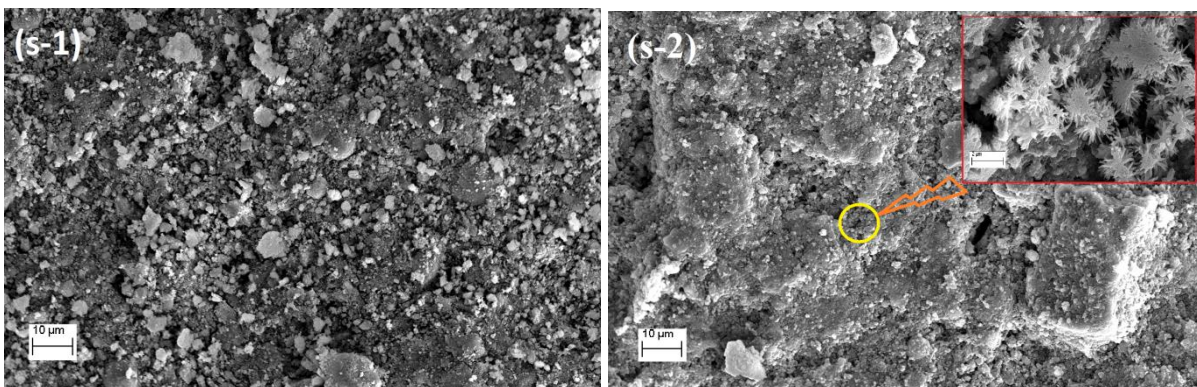


**Figure 8.10** Practically represent of bulk density of sample is lower than water.

**Table 8.2** Water absorption, expansion in water and thermal conductivity of cured CB samples.

Samples	Water absorption (%)		Expansion in water (%)		Thermal conductivity ( $\kappa$ ) (W/m·K)	
	Mean	s.d.	Mean	s.d.	30°C	200°C
s-1	26.36	0.68	0.12	0.01	0.102	0.153
s-2	18.76	0.38	0.11	0.02	0.171	0.216
s-3	21.03	0.42	0.11	0.02	0.144	0.203
s-4	23.54	0.37	0.10	0.02	0.129	0.188
s-5	24.89	0.56	0.10	0.02	0.116	0.164
s-6	21.64	0.46	0.37	0.04	0.162	0.206
s-7	22.83	0.31	0.63	0.06	0.149	0.183
s-8	24.95	0.52	1.23	0.08	0.112	0.164
s-9	22.77	0.44	0.33	0.04	0.128	0.171

Figure 8.11 exhibits the SEM micrographs of the fractured cross-sectional surface of cured CB specimens. SEM analyses demonstrate a low grade of densification with micro-pores for s-1 samples. It can be seen that the OPC addition has mark influenced on the microstructure of CB through the reduction of pore size and number of the pores, which may take place due to the formation of a higher amount of hydration products. Consequently, URHA incorporation does not create any large difference on microstructure. On the other hand, some micro-cracks are observed for RH containing samples. RH has a high tendency of moisture absorption, results to volume expansion. Therefore, cracks are developed in the body of CB specimens. Any detectable imperfection is not observed for the low amount of RH (5 wt.%) and 10 wt.% of URHA containing the sample.



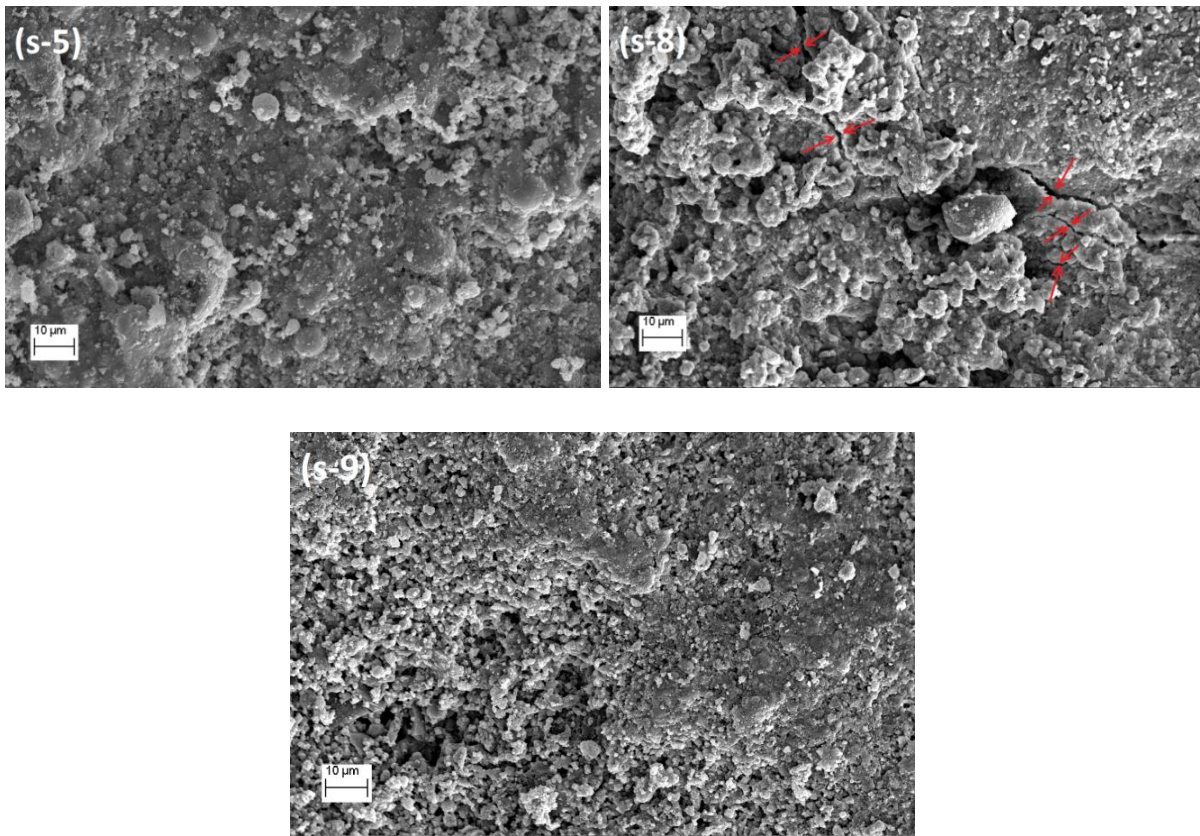


**Figure 8.11** SEM of cured ceramic board samples.

Table 8.2 shows the temperature dependence thermal conductivity of room temperature cured CB specimens and measurement is accomplished at temperatures of 30 and 200°C. It is found that the major phase of calcium silicate hydrate containing all CB samples show the lower value of  $\kappa$  because calcium silicate hydrate retain poorer values of  $\kappa$  (Leite *et al.*, 2017). However, the incorporation of OPC in the composition enhances the thermal conductivity coefficient. It may occur due to a decrease in the porosity of the samples. The unit weight is increased and crystalline hydration products also improve through this addition of OPC; as conformed by Figure 8.9(b) and Figure 8.6, respectively. On the contrary,  $\kappa$  values are decreased with the addition of URHA and RH in the composition. It may be happened due to lower  $\kappa$  values of the amorphous RHA silica (0.140 W/m·K) and organic fiber RH (0.035 W/m·K), which acts as a barrier to flow of heat; results drop in  $\kappa$  value (Gonzalves and Bergmann, 2007; Mishra *et al.*, 1986). It is also seen that the  $\kappa$  values are increased with the increasing measurement temperature of conductivity. Heat transfer through a solid happens via energy transfer between vibrating atoms by phonons, photons, electrons, ions, etc. For

insulating ceramic materials, phonons and photons are the key media for thermal conductivity; their contributions depend on the temperature mainly. At low temperatures, energy flow within a material occurs mainly via lattice vibrations (phonons) at a speed of sound. Consequently, the lattice vibrations are gradually increased with the increasing temperature in crystalline materials. It may be the reasons of thermal conductivity increment with temperature. While room temperature  $\kappa$  values of s-1 specimen is found to be 0.102 W/m·K and at 200°C, this specimen is offered  $\kappa$  value of 0.153 W/m·K.

Mechanical strength is a very vital index for the ceramic board because. It is required to withstand of most common stress, which are generally their own weight and handling under transport circumstances. The mean values of CCS and BS of different samples are illustrated in [Table 8.3](#), measured at room temperature after 28 days of sample preparation. The bending curves of some selective specimens are also shown in [Figure 8.12](#). It can be observed from [Table 8.3](#) that the strength values of both CCS and BS are greatly improved with the incorporation of OPC, URHA, and RH in the composition of CB. The improvement with OPC is due to the formation of a higher amount of hydration products, which are attributed to stronger bonds between different phases in CB ([Chen et al., 2017](#)). Moreover, lower porosity compares to only MCP containing (s-1) sample also play an important role in improving strength. In the non-ductile body, porosity induces a number of different promising sites for generating of cracks and its propagation ([Heriyanto et al., 2018](#)). Subsequently, URHA and RH in the system act as an aggregate or reinforcement media that increasing the stress resists capability and inhibits the crack propagation in the CB. The mechanism is graphically represented in [Figure 8.13](#). However, the strength value is reduced with URHA addition more than 15 wt.% in the composition. It may happen due to the reduction of hydrated products and an increase of brittle an-hydrated material (URHA). Consequently, RH has slightly more influence on BS than URHA. It may be due to RH, which is an organic fiber

and less brittle than URHA (Arjmandi *et al.*, 2015). Oppositely, RH has some drawback, such as high water absorption and volume expansion through moistening, which prevents its uses in higher amount (>10 wt.%) as a reinforcing agent. This expansion is introduced stress in the body and generated micro-cracks, as shown in Figure 8.11. Therefore, the strength value is reduced.

**Table 8.3** Cold crushing strength, bending strength and humidity effect on CCS of cured CB samples.

Samples	CCS (MPa)		BS (MPa)		CCS after humidity effect (MPa)		
	Mean	s.d.	Mean	s.d.	Mean	s.d.	HF (%)
s-1	7.27	0.21	3.33	0.13	6.83	0.22	-6.05
s-2	10.44	0.18	4.03	0.24	10.09	0.24	-3.35
s-3	12.68	0.27	6.12	0.21	12.22	0.29	-3.63
s-4	14.48	0.31	6.71	0.18	13.88	0.28	-4.14
s-5	13.84	0.43	6.59	0.35	13.16	0.38	-4.91
s-6	11.26	0.32	5.89	0.28	10.63	0.25	-5.56
s-7	13.57	0.30	8.14	0.34	12.38	0.29	-8.77
s-8	13.06	0.43	7.92	0.28	11.63	0.37	-10.95
s-9	14.39	0.27	7.41	0.21	13.62	0.29	-5.35

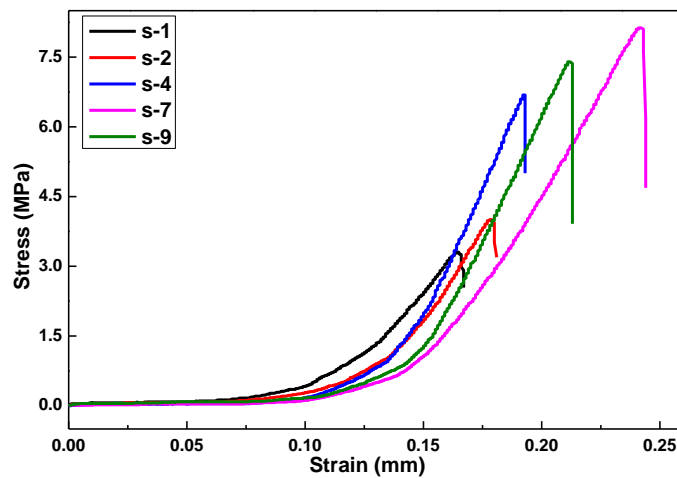


**Figure 8.12** Bending curve of ceramic board samples.

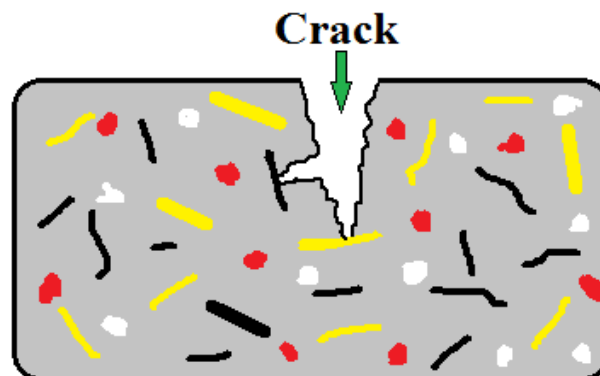


**Figure 8.13** Mechanism of mechanical strength of s-9 ceramic board sample.

The effect of humidity on the mechanical property (CCS) is an important parameter for board specimen in Indian weathering condition. The average relative humidity and temperature of some states in India during summer are above 60% and 40°C, respectively. Therefore, the experiment is done at 50°C temperature and 80% of relative humidity atmosphere. The CCS values after humidity treatment and percent of humidity effect are tabulated in [Table 8.3](#). The result demonstrates that the strength values for all samples are reduced. It may be happened due to absorb of moisture by capillary pores in the CB specimens at moistening environment. The absorbed moisture leads to a reduction of the cohesion forces between the particles and generates a diagonal bursting effect in the matrix of the CB composite. It is enhanced with an increase of the applied load ([Glücklich and Korin, 1975](#)). Therefore, the CCS of CB specimens is reduced. Addition to that, the swelling of wall particles by moisture increases the probability of cracking in CB. The absorbed moisture pressure with an applied compressive load on the capillary pore wall is another possible reason for the reduction of the strength in the moistening atmosphere ([Sathiparan and Rumeskumar, 2018](#)). Subsequently, the strength values are drastically reduced with RH incorporation in the composition. It may be ascribed due to volume expansion and high amount of moisture absorption by the RH containing samples ([Thakur and Gupta, 2006](#)).

From the above-evaluated characteristic, s-9 specimen exhibits optimum properties. The key properties of s-9 are compared with the obtained results from the literature using other wastes for the fabrication of CB, as shown in [Table 8.4](#). However, the acquired synthesis processes are different (not casting and room temperature curing process) like's high-temperature sintering and autoclaved curing method for the fabrication of CB using wastes. Thus, obtained results are huge different from our study. Additionally, the obtained results in s-9 are compared with the technical data of an international supplier company of calcium silicate board ([Leung, 2019](#)), as illustrated in [Table 8.5](#). It can be observed that the characteristics of waste derived CB are very good compared to the technical data of the



company. These promising characteristics and simple preparation method suggest that this work will open a new window to the calcium silicate board production industry for utilization of FA and seashell in the commercial production of CB.

**Table 8.4** Comparison of properties between s-9 sample and obtained data from the literature using other wastes.

References	Our sample (s-9)	Leite <i>et al.</i> (2017)	Felipe-Sese <i>et al.</i> (2011)	Carrasco-Hurtado <i>et al.</i> (2014)
Processes	Casting and room temperature curing	Pressing and curing	Sintering at 1100°C	Pressing and curing
Wastes	Seashells and FA	Chamotte and avian eggshells	Biomass ash and marble	Bottom ash
Density (gm/cc)	0.853 (Bulk density)	1.880 (Apparent density)	2.050 (Bulk density)	1.975 (Apparent density)
Thermal conductivity (W/m·K)	0.128	0.252	0.18	0.75
Water absorption (%)	22.77	14.38	8.5	10.25
Strength (MPa)	7.41 (Bending)	0.45 (Tensile)	58 (CCS)	61 (CCS)

**Table 8.5** Comparison of properties between s-9 sample and industry data.

Properties	Our sample (s-9)	Industry data (Leung, 2019)
Density (gm/cc)	0.853	0.950-1.150
Thermal conductivity (W/m·K)	0.128	≤0.22
Water absorption (%)	22.77	≤42
Bending strength (MPa)	7.41	4-6

## 8.4 Summary

Depending on the results obtained in this study, it can be concluded that the seashells and fly ash can be used as ingredients for the fabrication of the sustainable ceramic board. It can be used for the lining inside the rooms for thermal insulation. The physical, thermal and mechanical characteristics of CB have been examined. It is found that the 1100°C calcined seashells and fly ash mixture contained larnite ( $\text{Ca}_2\text{SiO}_4$ ) is a major phase; and mullite

( $\text{Al}_{4.56}\text{Si}_{1.44}\text{O}_{9.72}$ ), calcium aluminate ( $\text{Ca}_3\text{Al}_2\text{O}_6$ ) and anorthite ( $\text{CaAl}_2\text{Si}_2\text{O}_8$ ) are minor phases. The hydration products of the ceramic board (CB) are calcium silicate hydrate ( $\text{Ca}_6\text{H}_2\text{O}_{13}\text{Si}_3$ ), tanzanite ( $\text{Ca}_2\text{Al}_2\text{Si}_3\text{O}_{12}\text{OH}$ ) and calcium aluminum oxide hydrate ( $\text{Ca}_4\text{Al}_2\text{O}_7 \cdot 19\text{H}_2\text{O}$ ), which are responsible for the strength of the board. The multi-phase ceramic powder containing board specimens are demonstrated a lower density, low thermal conductivity, and good mechanical strength. OPC, URHA and RH incorporation in the composition are strongly influenced the physical and mechanical properties of CB. URHA does not significantly alter the physical characteristic, but RH addition enhances the water absorption and expansion behavior of CB specimens. The mechanical properties of CB are improved with the addition of URHA and RH in the composition up to a limit, i.e.  $\leq 15$  wt.% URHA and  $\leq 10$  wt.% RH. RH containing samples exhibit mark influences through the humidity atmosphere and reduce the strength value of samples.